

INFORMATION TO USERS

While the most advanced technology has been used to photograph and reproduce this manuscript, the quality of the reproduction is heavily dependent upon the quality of the material submitted. For example:

- Manuscript pages may have indistinct print. In such cases, the best available copy has been filmed.
- Manuscripts may not always be complete. In such cases, a note will indicate that it is not possible to obtain missing pages.
- Copyrighted material may have been removed from the manuscript. In such cases, a note will indicate the deletion.

Oversize materials (e.g., maps, drawings, and charts) are photographed by sectioning the original, beginning at the upper left-hand corner and continuing from left to right in equal sections with small overlaps. Each oversize page is also filmed as one exposure and is available, for an additional charge, as a standard 35mm slide or as a 17"x 23" black and white photographic print.

Most photographs reproduce acceptably on positive microfilm or microfiche but lack the clarity on xerographic copies made from the microfilm. For an additional charge, 35mm slides of 6"x 9" black and white photographic prints are available for any photographs or illustrations that cannot be reproduced satisfactorily by xerography.



8716348

Brikowski, Tom Harry

A QUANTITATIVE ANALYSIS OF HYDROTHERMAL CIRCULATION AROUND
MID-OCEAN RIDGE MAGMA CHAMBERS

The University of Arizona

PH.D. 1987

University
Microfilms
International 300 N. Zeeb Road, Ann Arbor, MI 48106



PLEASE NOTE:

In all cases this material has been filmed in the best possible way from the available copy. Problems encountered with this document have been identified here with a check mark .

1. Glossy photographs or pages _____
2. Colored illustrations, paper or print _____
3. Photographs with dark background _____
4. Illustrations are poor copy _____
5. Pages with black marks, not original copy _____
6. Print shows through as there is text on both sides of page _____
7. Indistinct, broken or small print on several pages
8. Print exceeds margin requirements _____
9. Tightly bound copy with print lost in spine _____
10. Computer printout pages with indistinct print _____
11. Page(s) _____ lacking when material received, and not available from school or author.
12. Page(s) _____ seem to be missing in numbering only as text follows.
13. Two pages numbered _____. Text follows.
14. Curling and wrinkled pages _____
15. Dissertation contains pages with print at a slant, filmed as received _____
16. Other _____

University
Microfilms
International



A QUANTITATIVE ANALYSIS OF HYDROTHERMAL CIRCULATION
AROUND MID-OCEAN RIDGE MAGMA CHAMBERS

by
Harry
Tom Brikowski

A Dissertation Submitted to the Faculty of the
DEPARTMENT OF GEOSCIENCES
In Partial Fulfillment of the Requirements
For the Degree of
DOCTOR OF PHILOSOPHY
In the Graduate College
THE UNIVERSITY OF ARIZONA

1987

THE UNIVERSITY OF ARIZONA
GRADUATE COLLEGE

As members of the Final Examination Committee, we certify that we have read
the dissertation prepared by Tom Harry Brikowski
entitled A Quantitative Analysis of Hydrothermal Circulation Around
Mid-Ocean Ridge Magma Chambers

and recommend that it be accepted as fulfilling the dissertation requirement
for the Degree of Doctor of Philosophy.

<u>[Signature]</u>	<u>13 April 1987</u> Date
<u>[Signature]</u>	<u>13 April 1987</u> Date
<u>[Signature]</u>	<u>13 April 1987</u> Date
<u>[Signature]</u>	<u>"</u> Date
<u>[Signature]</u>	<u>13 Apr 87</u> Date

Final approval and acceptance of this dissertation is contingent upon the
candidate's submission of the final copy of the dissertation to the Graduate
College.

I hereby certify that I have read this dissertation prepared under my
direction and recommend that it be accepted as fulfilling the dissertation
requirement.

<u>[Signature]</u>	<u>Apr 1987</u>
Dissertation Director	Date

STATEMENT BY AUTHOR

This dissertation has been submitted in partial fulfillment of requirements for an advanced degree at the University of Arizona and is deposited in the University Library to be made available to borrowers under rules of the Library.

Brief quotations from this dissertation are allowable without special permission, provided that accurate acknowledgement of source is made. Requests for permission for extended quotation from or reproduction of this manuscript in whole or in part may be granted by the head of the major department or the Dean of the Graduate College when in his or her judgement the proposed use of the material is in the interests of scholarship. In all other instances, however, permission must be obtained from the author.

SIGNED: Tom Bilaski

ACKNOWLEDGEMENTS

The development of the general flow-modeling code used in this study was funded by the State of Arizona through a Geohydrology grant to Dr. Norton. The modeling itself was funded in part through an NSF grant to Dr. Norton, and indirectly by the SCS Corporation during the beta-testing stage of their min-Cray. Generous support in my first years was provided by a Chevron Fellowship and the Department of Geosciences. Crucial indirect support was provided by Denis Norton in giving me complete access to his excellent computational laboratory facilities. My personal thanks go to Denis, who reviewed numerous early versions of this dissertation, and who together with Randy Richardson provided much useful guidance in the black art of modeling non-linear systems.

Thanks go to a number of fellow students, including Jim Johnson, whose influence was critical in my study, and to Regina Capuano for keeping Jim and me out of the doghouse for so long. Steve Sorenson wrote and maintained all of the graphics routines used in this effort, work in the future will be impossible without him. Others made graduate life more tolerable, including Glenn Grant and Nancy Hess, who always kept me posted on the status of the official gin and tonic season; Dianne Marozas and her undying faith in the Cubs; and the GBO, who always made me keep academics in perspective. Finally, a special thanks to Jean Cline for all the good times, at least until she ran off with Bob.

This dissertation is dedicated to Jerry Knight.

TABLE OF CONTENTS

	Page
LIST OF ILLUSTRATIONS	vi
LIST OF TABLES	vii
ABSTRACT	viii
1. INTRODUCTION	1
Mid-Ocean Ridge Environment	2
Tectonics	2
Magmatism	2
Hydrothermal Circulation	4
2. METHOD OF INVESTIGATION	6
Model Equations	7
Solution Methods	9
Material Properties	11
Fluids	11
Rock	11
Choice of Models	14
3. NARROW CHAMBER	15
P-T-v History	15
1,000 yrs	19
1,000-20,000 yrs	19
30,000-50,000 yrs	25
50,000-70,000 yrs	25
Summary	26
4. WIDE CHAMBER	28
P-T-v History	28
0-30,000 yrs	32

TABLE OF CONTENTS—Continued

	Page
30,000-70,000 yrs	36
70,000-170,000 years	37
Summary	38
 5. DISCUSSION	 39
Spreading and Multiple Intrusions	40
Fracture Zones	41
 6. CONCLUSIONS	 43
 APPENDIX A: GLOSSARY OF SYMBOLS	 45
 REFERENCES	 47

LIST OF ILLUSTRATIONS

1.	Narrow chamber geometry	16
2.	Narrow chamber element grid and boundary conditions.	17
3.	Narrow chamber, mass flux at the ocean floor for selected times. . .	18
4.	Narrow chamber : Fluid heat capacity and velocity at 1,000 yrs. . .	20
5.	Narrow chamber: T contours, \mathbf{v} vectors, and time-integrated mass flux contours for selected times.	22
6.	Narrow chamber : Temperature vs. depth at the ridge axis.	24
7.	Comparison of initial geometries, wide and narrow chambers.	29
8.	Wide chamber : Element grid.	30
9.	Wide chamber : mass flux at the ocean floor for selected times.	31
10.	Wide chamber : Fluid heat capacity contours and \mathbf{v} at 10,000 yrs.	33
11.	Wide chamber: T contours, \mathbf{v} vectors, time-integrated mass flux and streamfunction contours at selected times.	34

LIST OF TABLES

1.	Solution sequence.	10
2.	Summary of intrinsic material properties used in models.	13

ABSTRACT

Hydrothermal activity is one of the dominant processes affecting the chemical and thermal evolution of oceanic crust at the mid-ocean ridge (MOR), but little is known about the sub-surface portions of ridge hydrothermal systems. These systems can be investigated using numerical modeling techniques, and models of two-dimensional cross-sections are utilized in this study to investigate the behavior of MOR hydrothermal systems. The influence of magma chamber geometry is explored by modeling two extremes of proposed geometry.

Seismological evidence supports a dike-like 2 km half-width chamber, and models of this chamber indicate that : 1) complete crystallization of the magma requires 30,000 years, 2) hydrothermal upflow and hot springs are concentrated in a narrow band within 1.5 km of the ridge axis for the lifetime of the system, 3) a large hydrothermal cell forms and remains centered above the distal tip of the intrusion for the lifetime of the system, 4) effective hydrothermal activity ends by 70,000 yrs.

Petrological evidence supports a wide sill-like chamber 15 km in half-width, and models of this chamber indicate that : 1) complete crystallization of the magma requires 100,000 yrs, 2) hydrothermal vents are present at the ridge axis, but most of the vents are located 5-10 km away from the axis, 3) a large hydrothermal cell develops at the distal tip of the magma chamber, while a series of small but vigorous cells develops directly above the intrusion, both features migrate toward the ridge axis as the magma solidifies, 4) effective hydrothermal activity ends by 170,000 yrs.

Substantially different hydrothermal systems develop around these two chamber geometries and comparison of the models shows this is because different patterns of near-critical P-T conditions developed around them. The fundamental influence on the nature and pattern of hydrothermal circulation at MOR is the distribution of near-critical conditions.

CHAPTER 1

INTRODUCTION

Hydrothermal activity is a fundamental geologic process at mid-ocean ridges, and has a major influence on the evolution of oceanic crust and ocean water; unfortunately, little is known about the nature and pattern of ridge hydrothermal systems, especially their sub-surface portions. Without this knowledge a wide variety of geologic features and phenomena at mid-ocean ridges must remain poorly understood. The problem is particularly acute in the study of sea-floor hot springs, whose characteristics, distribution in space and time, and evolution depend entirely on the nature of sub-surface flow. The magnitude and distribution of by-products of ridge hydrothermal activity obviously depend on the nature of sub-surface flow, and these by-products include ore deposits, chemical and isotopic alteration of ocean crust and seawater, and heat and chemical transport in general. This study is intended to fill in some of this missing information through the application of numerical modeling techniques to investigate the nature of sub-surface hydrothermal circulation at mid-ocean ridges and the major factors influencing it.

Hydrothermal circulation is inevitable whenever magmas intrude permeable, fluid saturated rocks. Mid-ocean ridges are the sites of the most continuous and voluminous magmatic activity on the Earth, and therefore they are also the sites of the most continuous and voluminous hydrothermal activity on the Earth. Because of this strong correlation, particular attention will be paid in this study

to the influence of magmatic activity on the nature of hydrothermal activity at mid-ocean ridges.

Mid-Ocean Ridge Environment

The ridge environment has received a tremendous amount of scientific attention, and much is known about the geology and dynamics of mid-ocean ridges. This data-base provides the basic constraints for numerical models. Excellent general reviews have been written by Lewis(1983) and MacDonald(1986).

Tectonics

Mid-ocean ridges are the sites of sea-floor spreading, and new oceanic crust is repeatedly created at the ridge axis. The axes are divided into separate spreading segments, connected by transform faults. A typical ridge segment is 50 km long in the Atlantic, spreading episodically (events every 10,000-50,000 yrs) at an average rate of 2 cm/yr (MacDonald 1986). At slow spreading centers like the mid-Atlantic ridge the crest of the ridge is marked by an axial graben up to 60 km wide and 1-3 km deep. In the Pacific spreading rates are 6-9 cm/yr, ridge segments are longer (40-140 km long), and the central rifts are replaced by axial highs 8-20 km wide and 200-400 m high (MacDonald, Sempere and Fox 1984). Fast spreading ridges develop axial grabens near transform faults, apparently in response to decreased magma supply at the distal ends of each ridge segment, providing clear evidence for along-axis variability in ridge characteristics (MacDonald 1986).

Magmatism

Magmatic activity is the crust-forming mechanism at mid-ocean ridges. Detailed studies at the ridge axis indicate that igneous activity is episodic, with

new eruptions occurring at the surface every 10,000-50,000 yrs in the Atlantic, producing a discontinuous neo-volcanic zone 1-3 km wide (MacDonald 1986). Fast spreading ridges have a nearly continuous but equally narrow neo-volcanic zone (MacDonald, Sempere and Fox 1984). Rates of magma intrusion from the mantle into the crust are unknown, but can be estimated from mass-balance considerations. The maximum interval between intrusions can be calculated by assuming a size for the magma chamber, and that the chamber fills completely and instantly, with no further additions of magma until the next chamber forms. Given these assumptions, to maintain a half spreading rate of 2 cm/yr would require intrusions every 270,000 years for large chambers (see below) and 50,000 years for small chambers. Similar considerations have been used to argue that a steady-state magma chamber should be present at intermediate to fast spreading rates (Sleep and Rosendahl 1979, Sleep 1983).

Investigations at the ridge axis indicate that magma bodies are small. Seismic studies reveal zones of marked attenuation capped by shallow reflectors beneath the ridge crest. These features are thought to represent the body and top (respectively) of magma chambers, extending no more than 2 km away from the ridge axis (Detrick et al. 1986, McClain, Orcutt, and Burnett 1985). In addition, petrologic studies of ridge crest basalts reveal large local compositional variations, indicating that they were derived from discrete magma bodies (Bryan and Moore 1977, Langmuir, Bender, and Batiza 1986) or source regions (Shirey, Bender, and Langmuir 1987).

In contrast, data from ophiolites suggest large magma chambers form at the ridge; for the Oman ophiolite a 15 km half-width magma chamber has been proposed (Pallister and Hopson 1981, Gregory and Taylor 1981). Laterally extensive cumulate layers and lack of cross-cutting relationships in the cumulate gabbros

support the concept of a large chamber, and lack of cryptic (compositional) variation in the cumulates suggests a steady-state chamber. More recently it has been suggested that the Oman rocks were generated by a series of laterally extensive (5-6 km half-width) sills (R. Gregory, pers. commun., 1987).

Hydrothermal Circulation

The existence of sea-floor hot springs on several ocean ridges provides direct evidence of the widespread occurrence of hydrothermal activity (Corliss et al. 1979, Rona et al. 1986) and studies of these springs provide useful constraints on ridge hydrothermal processes. These springs typically occur in several clusters of vents comprising a hydrothermal field. Each cluster occupies an area approximately 100x100 m, while the entire field can be up to half a kilometer wide and several kilometers long (Francheteau and Ballard 1983). Known hot springs are restricted to the neovolcanic zone in the axial valleys of the mid-ocean ridges; none have been found off the ridge axis.

Other studies demonstrate that hydrothermal activity is widespread away from the ridge axis, and may extend below the base of the crust. The development of multiple convection cells for distances up to 200 km from the ridge axis is indicated by the periodic nature of measured heat flow values along sections perpendicular to the axis (Williams, vonHerzen, Sclater, et al., 1974; Ribando, Torrance & Turcotte, 1976; Wolery & Sleep 1976). Recent studies suggest that much hydrothermal activity takes place off the ridge axis (Morton and Sleep 1985, Bowers and Taylor 1985). The pervasive nature of chemical and isotopic alteration observed in ophiolites indicates that hydrothermal activity has a large vertical extent (Spooner et al. 1977, Gregory and Taylor 1981), and the discovery by Gregory and Taylor of oxygen-isotopic alteration in former

mantle rocks at the base of the Oman ophiolite suggests that this hydrothermal activity penetrates the base of oceanic crust.

A number of thermal models have been proposed for mid-ocean ridges, and most include some estimate of hydrothermal activity. The most successful of these use heat and mass-balance considerations to calculate net fluid fluxes at the ridge, without regard to the pattern of sub-surface fluid flow. For example, measurements of sea-floor heat flow show that hydrothermal activity dissipates two-thirds of all magmatic heat released at the mid-ocean ridges (Lister 1972). This in turn implies that a volume of sea water equivalent to the entire volume of Earth's oceans must pass through and interact with the oceanic crust over a period of 5-10 million years (Wolery and Sleep 1976). Chemical models produce similar results based on global chemical balances (Wolery and Sleep 1976, Thompson 1983) and local balances (Bowers and Taylor 1985).

Several studies investigate the pattern and distribution of fluid and heat transport in oceanic environments. Gartling (1982) studied fluid convection in oceanic sediments, and Williams, Narasimhan, Anderson, et al. (1986) present a flow model for the vicinity of a DSDP borehole on the Costa Rica Rift. Fehn & Cathles (1979) published a model for the entire thickness of oceanic crust at the ridge in which somewhat arbitrary permeability channels controlled fluid flow, and Cathles(1983) has modeled hydrothermal circulation in Kuroko (silicic back-arc) environments. Morton and Sleep (1985) discuss the heat sink/source constraints of hydrothermal flow in a unique modeling application, concluding that fluid flow profoundly influences magma chamber shape.

CHAPTER 2

METHOD OF INVESTIGATION

Direct observation of the sub-surface portions of hydrothermal systems is extraordinarily difficult, and is virtually impossible at mid-ocean ridges. Instead, we must study analogs to the ridge hydrothermal systems; these can take the form of physical or numerical models. Numerical models offer the advantage of extreme flexibility, and for that reason they are employed in this study.

Fluid flow and heat transport in geologic settings can be described using mathematical statements of the conservation laws for heat, mass, and momentum. These statements can be manipulated to obtain equations for the dependent variables temperature and pressure, which can then be solved to obtain T and P at any point and time in the model system. Finally, derivative quantities such as fluid velocity and fluid properties can be obtained as functions of computed T and P. The basic conservation laws describe balances at a point, but can be extended to describe a continuum by treating all quantities as averages over a discrete portion of the continuum, or Representative Elemental Volume (REV). All quantities in the discussion below represent volume averages, or phase averages for fluid properties, and the equations represent balances over an REV. The detailed derivation of the equations governing fluid flow in geologic settings is available in numerous sources (Norton and Knight 1977, Norton, unpubl. manuscript 1987) and will not be repeated here.

Some simplifying assumptions are helpful. To simplify the form of the basic equations , the effects of changes in fluid density will not be considered except

where they affect fluid buoyancy (i.e. the fluid is assumed to be incompressible in most cases). A second assumption is that fluids are in thermal equilibrium with their host rocks at all times ($T_f = T_s$), a reasonable approximation since thermal conductivity is much higher for fluids than for rock.

Some simplifications can be made regarding the problem domain as well. Ridge chambers extend for large distances along the ridge axis, and only a short distance away from the axis, consequently the system can be approximated by a two-dimensional section perpendicular to the axis which requires that little heat flow occurs along the ridge axis. Taking the chamber to be symmetric about the ridge axis (note actual spreading appears to be asymmetric in the short term; MacDonald, 1986), the model can be limited to a semi-infinite half-space bounded by the ridge axis.

Model Equations

Heat is the energy source driving fluid flow in hydrothermal systems, and the mathematical statement of heat conservation provides the fundamental equation in this development. This conservation equation relates the change in heat content of the REV to the amount of heat carried across the boundary of the REV by conduction and convection. Expressing heat in the system as $\rho c_p T$ (Norton and Knight 1977) and assuming the fluid to be incompressible, conservation of heat can be written using the differential form of the transport theorem

$$\underbrace{\rho(c_p + Q_{zl}) \frac{\partial T}{\partial t}}_{\text{content}} - \underbrace{\nabla \kappa \cdot \nabla(\rho c_p T)}_{\text{conduction}} + \underbrace{\mathbf{v} \cdot \nabla(\rho c_p T)}_f = 0 \quad (2.1)$$

The latent heat of crystallization, Q_{zl} , comprises about one-third of the total heat content of mafic magmas, and is incorporated directly into the heat-content term

of (2.1). Equation (2.1) is in reality a temperature equation since heat has been expressed as a function of T.

A statement similar to (2.1) can be written to describe conservation of fluid mass

$$\frac{\partial \rho}{\partial t} + \nabla \cdot (\rho \mathbf{v}) = 0 \quad (2.2)$$

If the fluid is assumed to be incompressible (i.e. ρ_f is invariant in space and time), (2.2) reduces to

$$\nabla \cdot \mathbf{v} = 0 \quad (2.3)$$

This equation has already been applied to (2.1) to simplify the convective term.

The third conserved quantity in these models is fluid momentum, and for an incompressible fluid, extending the expression for momentum conservation to apply to continua results in Darcy's Law

$$\mathbf{v} = -\frac{k}{\mu} (\nabla P + \rho_f \mathbf{g}) \quad (2.4)$$

which assumes a steady-state flow field. An expression for pressure can be obtained by applying (2.3) to (2.4)

$$\nabla \cdot \left(\frac{k}{\mu} \nabla P \right) = -g \frac{\partial}{\partial z} \left(\frac{k \rho_f}{\mu} \right) \quad (2.5)$$

where z is the vertical coordinate and is positive upward. This equation is also steady-state, owing to the nature of its derivation. In (2.5) changes in pressure depend only on fluid properties, contributions from the rock matrix are not specifically included.

Fluids in the system are approximated by pure H₂O, and their properties are computed as continuous functions of T and P using the extremely accurate equations presented by (Haar, Gallagher, and Kell 1980, Levelt Sengers, et al. 1983) (computer program

H2O84, Johnson, 1987). This adds a fourth equation to the basic equations of the model, the equation of state for pure H_2O .

Solution Methods

Given initial and boundary conditions, equations (2.1) and (2.5) can be integrated over space and time to give the transient temperature and resulting steady-state pressure fields at any time for the model system. The steady-state velocity field can then be obtained using (2.4) (Table 1). The finite element method is used to perform the spatial integration in these models, employing quadratic triangular elements, and using the modified backward implicit approximation for time-integration (Lapidus and Pinder 1982 , p. 283). The modified backward method treats time-derivative terms with a time-centered difference approximation, and space-derivative terms with a backward difference in time. Program MARIAH was used to compute the models, a code originally developed by Gartling(1982) and extensively modified in our laboratory to include an accurate equation of state for H_2O , and to reflect the dependent variable formulation outlined above.

The strong dependence of fluid properties on pressure and temperature makes (2.1) and (2.5) a highly non-linear set of equations (i.e. the coefficients in these equations depend directly on the variables). The solution sequence (Table 1) treats this non-linearity by introducing a lag of one time step, computing fluid properties at the n th time step as functions of the conditions at the previous time step. Even with this lag, the non-linear nature of (2.1) and (2.5) can introduce solution instability for large time steps because heat convection can outpace the numerical rate of propagation in the model. In the finite element formulation, heat can move only from an element to its neighbor during a time step; therefore

Table 1: Solution sequence.

For the n th time step quantities are computed in the order listed, where first fluid properties, then T , P and \mathbf{v} are solved for (i.e. equations (2.1), (2.5), and (2.4) are solved sequentially at each time step). Superscript represents time-step number, subscript f indicates fluid property.

	Computed quantity	as a function of	using equation
1	new fluid properties $(\rho, c_p, \mu, \kappa)_f^n$	last T & P (T^{n-1}, P^{n-1})	
2	new T T^n	new fluid props., last T & \mathbf{v} $(\rho, c_p, \mu, \kappa)_f^n, T^{n-1}, \mathbf{v}^{n-1}$	(2.1)
3	new P P^n	new fluid props. $(\rho, c_p, \mu, \kappa)_f^n$	(2.5)
4	new \mathbf{v} \mathbf{v}^n	new fluid props., P $(\rho, c_p, \mu, \kappa)_f^n, P^n$,	(2.4)

$\Delta x_i/\Delta t$ defines a maximum numerical velocity, and true velocity must be less than or equal to the numerical velocity to avoid solution errors. In this study, the instability problem was avoided by selecting time steps such that $\Delta x_i/\Delta t \geq |v_i|$ known also as a Courant restriction (Huyakorn & Pinder, 1983, p. 206; Roache, 1972, p. 41).

Material Properties

Fluids

The properties of H₂O -rich fluids vary in a highly non-linear fashion in the critical region of H₂O , and this critical behavior has a profound impact on hydrothermal systems (Norton, 1984). The transport properties reach extrema in the vicinity of the critical point, causing fluid flux and heat transport to be maximized. Fluid flux is maximized in the critical region because viscosity reaches a minimum, and the gradient of fluid density in P-T space becomes large. Recall that fluid velocity is equal to the force per unit volume acting on the fluid (pressure force+gravitational force), multiplied by a proportionality constant k/μ (2.4). Critical conditions maximize fluid forces by enhancing the likelihood that ∇P and $\rho_f \mathbf{g}$ will be out of balance as ρ_f becomes extremely variable, and by increasing the size of the proportionality constant in (2.4). Fluid heat capacity reaches a sharp maximum under these same conditions, and this maximum in heat carrying capacity combined with the maximum in fluid velocities results in an enormous increase in convective heat transport in the critical region.

Rock

Properties of the matrix, especially permeability, have an important influence on fluid circulation. Unfortunately, permeability is one of the most variable and least constrained rock properties. Values used in this study (Table 2) are based on estimates for the Skaergaard Intrusion (Norton and Taylor 1979) and DSDP measurements (Anderson et al. 1985). Estimates of flow porosities consistent with these permeabilities were determined using total porosity and fracture density data from Anderson, et al. and MacDonald (1986). Lateral permeability variations are undoubtedly present at the mid-ocean ridges, particularly in association with tectonic movements along the axial valley, but specific knowledge of their distribution is lacking; therefore permeabilities are treated as uniform and isotropic within each geologic unit in the models below.

The nature of the intrusive rocks is also important. In models below the magma intrudes at 1250°C, just below its liquidus temperature (Usselman and Hodge 1978) and remains impermeable until it cools to 100°C below its solidus temperature. Upon reaching that temperature, the intrusive rocks are assumed to instantly acquire a fracture permeability (Knapp and Norton 1981) equivalent to that of the surrounding gabbros. The magma adds significant heat to the system in the form of latent heat of crystallization, and the distribution of this heat is an important variable. Petrologic evidence indicates that the final melt fraction (hence the bulk of crystallization heat) is found in the upper parts of mid-ocean ridge magma chambers, and therefore this heat source is concentrated near the top of the magma chamber in the models.

A background geothermal gradient of $\sim 180^{\circ}\text{C}/\text{km}$ is assumed, consistent with heat flow measurements (Becker, et al., 1985) and a mantle at near-liquidus temperatures for mid-ocean ridge basalts. To simplify the models, the chambers

Table 2: Summary of intrinsic material properties used in models.

Data from Usselman & Hodge, 1978; Clark, 1966.

All Solids

	heat capacity	c_p	0.25	cal/gr °C
	thermal conductivity	κ	0.0068	cal/cm sec °C
<u>Magma</u>				
	$T_{intrusion}$		1250	°C
	$T_{solidus}$		1150	°C
	$T_{fracture}$		1050	°C
	latent heat of crystallization	Q_{zl}	100	cal/cm ³ °C
	density	ρ	3.0	gm/cm ³
	flow porosity	ϕ	0.48e-5	
	permeability (initial)	k	10 ⁻¹⁹	cm ²
<u>Basalt/Dikes</u>				
	density	ρ	2.7	gm/cm ³
	flow porosity	ϕ	0.48e-3	
	permeability	k	10 ⁻¹²	cm ²
<u>Gabbro</u>				
	density	ρ	3.0	gm/cm ³
	flow porosity	ϕ	0.48e-5	
	permeability	k	10 ⁻¹³	cm ²
<u>Mantle</u>				
	density	ρ	3.3	gm/cm ³
	flow porosity	ϕ	0.48e-8	
	permeability	k	10 ⁻¹⁴	cm ²

are assumed to be products of a single, instantaneous intrusive event; the effects of sea-floor spreading (matrix advection) are not included. The consequences of these simplifications are minor, and are discussed later.

Choice of Models

The two lines of geological evidence outlined in Chapter 1 imply substantially different magma chamber geometries at the mid-ocean ridges. These extremes in chamber geometry will produce substantially different force fields for fluid flow, and consequently will develop profoundly different hydrothermal systems. Both extremes will be modeled in this study in order to directly examine the effects of magma chamber geometry on hydrothermal activity at the mid ocean ridges.

CHAPTER 3

NARROW CHAMBER

The narrow dike-like chambers proposed from seismic evidence represent the minimum probable size for chambers at the ridge axis. McLain, Orcutt & Burnett (1985) present a cross-section of such a magma chamber extending 2 km from the ridge axis and 4 km vertically, and this is the basis of the narrow model (Fig.1). Initial and boundary conditions for the model are summarized in Figs. 2 and 1, the various material properties used in the model are summarized in Table 2. The problem domain was divided into 376 elements using 909 nodes, a total of 95 time steps was required to complete the solution. Heat sources were concentrated between 1.25 and 1.75 km depth.

P-T-v History

The history of hydrothermal circulation around the narrow chamber can be divided into three stages based on the magnitude of convective heat and fluid transport above the magma chamber. From 0-20,000 years convective heat transport increases rapidly, from 20,000-50,000 years it reaches a peak and remains high, and from 50,000-70,000 years it declines slowly, reaching low values by 70,000 years. This history is reflected in the variation of fluid flux at the surface (Fig.3).

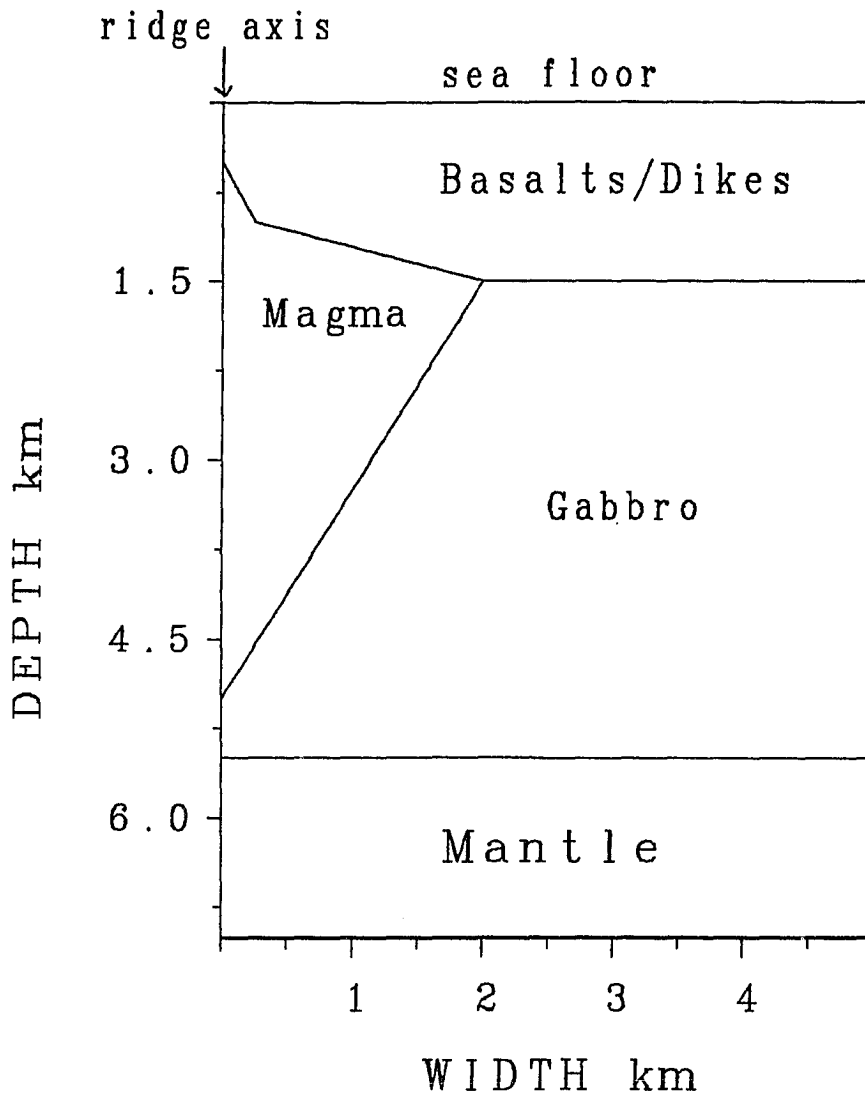


Figure 1: Narrow chamber geometry

Cross-section showing distribution of lithologic units. Permeabilities and other properties are summarized in Table 2.

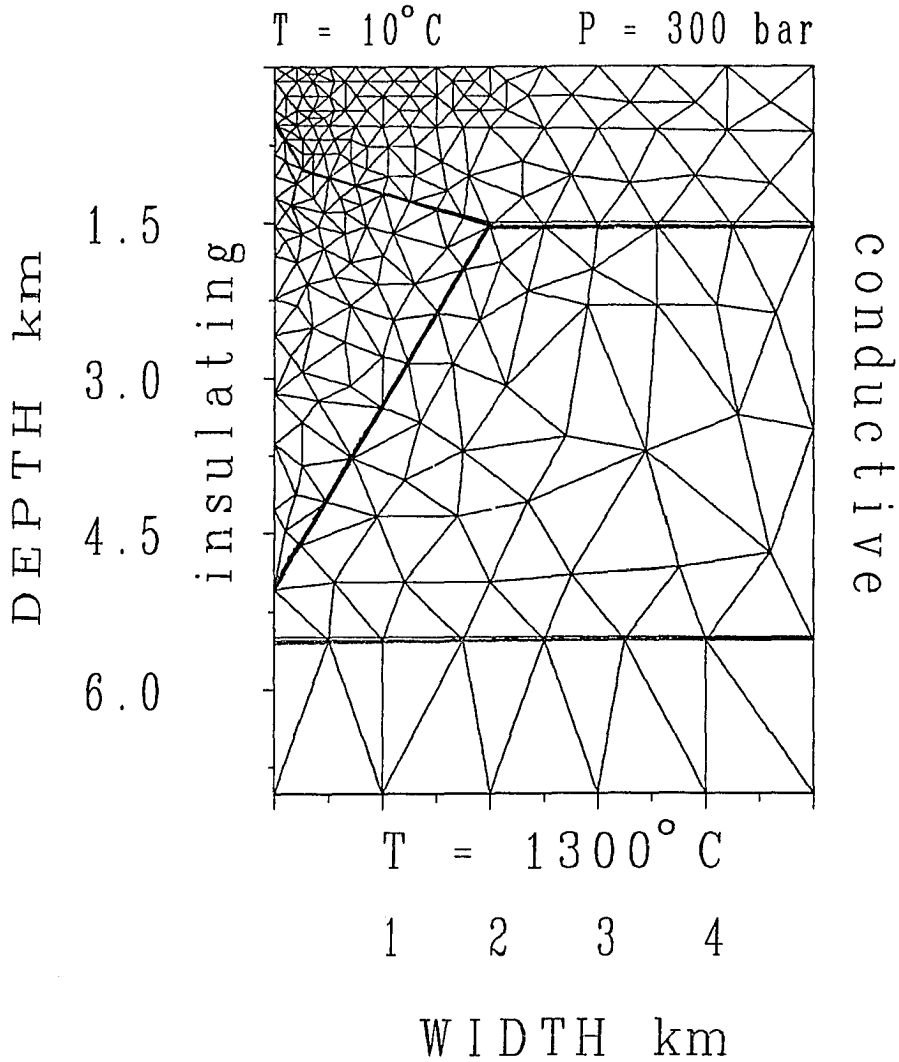


Figure 2: Narrow chamber element grid and boundary conditions.

Cross-section showing distribution of finite elements and imposed boundary conditions. No heat or fluid is allowed to pass through the left side of the problem domain, heat and fluid can pass through the remaining sides. Temperature is held at background values on the right side of the domain.

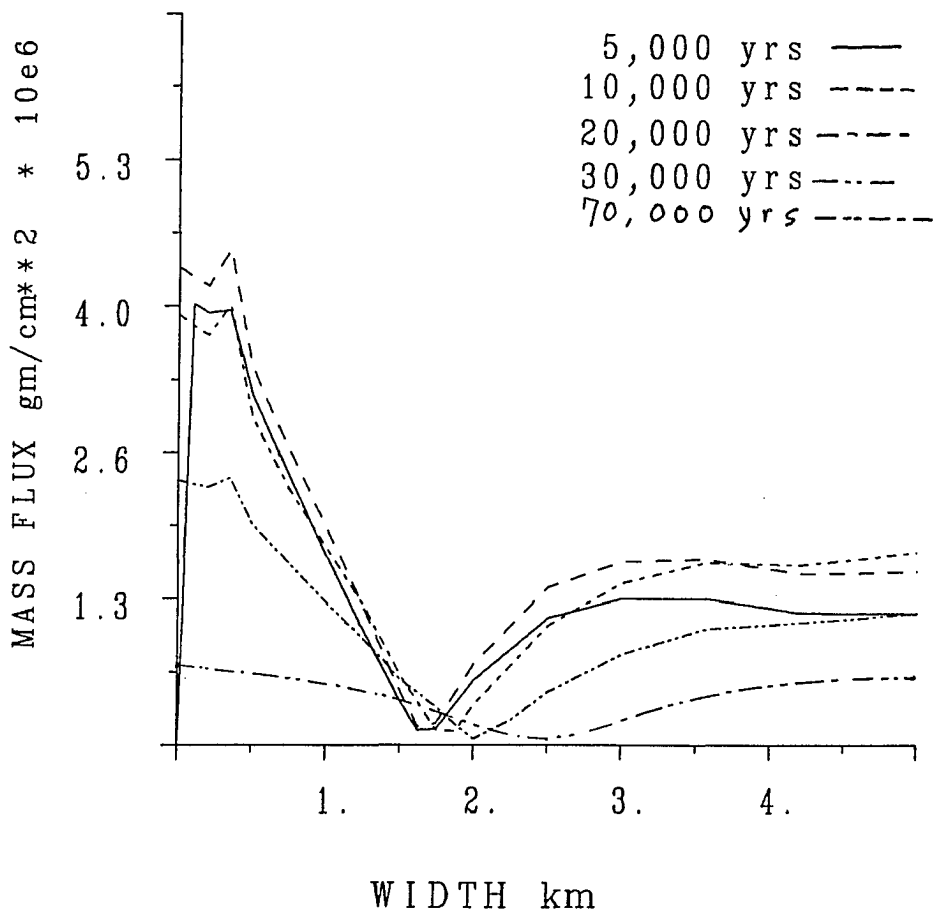


Figure 3: Narrow chamber, mass flux at the ocean floor for selected times. Instantaneous mass flux ($\rho \cdot |v|$) at 5,000, 10,000, 30,000 and 70,000 years. Mass flux declines rapidly after 20,000 years. Fluid flow is downward at distances greater than 2 km from the ridge axis.

1,000 yrs

The control of fluid properties on the distribution of maximum velocities is already apparent at 1000 years. A small region of near-critical conditions forms just above the intrusion along the ridge axis, and maximum velocities are found in that region (Fig.4). The peak buoyancy forces and minimum viscosities are found in this small zone above the intrusion, and consequently fluids acquire a strong vertical velocity component and move rapidly out of the top of the zone. They are replaced by fluids lying farther from the ridge axis which are drawn into the bottom of the zone. Upflow is strongly focused at the ridge axis because of the tendency of fluids to be attracted to this zone. Critical conditions are not enough to insure high fluid velocities however, fluid forces must be non-zero as well. A broad region of moderately critical conditions is found at 2 km depth in the distal gabbros, but here conditions are stable, fluid forces are balanced, and in spite of the moderately critical conditions, high fluid fluxes are not present.

1,000–20,000 yrs

The magma decreases to three-fourths its original volume by 5,000 years (Fig.5), with crystallization proceeding most rapidly at the distal tip where high surface area makes conductive heat loss most rapid. Half the magma remains by 10,000 years, and by 20,000 years only 20% remains. The outer portions of the intrusion rapidly cool to the fracture temperature, and hydrothermal fluids begin to circulate in much of the outer part of the intrusion by 20,000 years. Buoyant fluids traveling upward through the intrusion are deflected around the remaining magma, but by 20,000 years only a small part of the intrusion remains

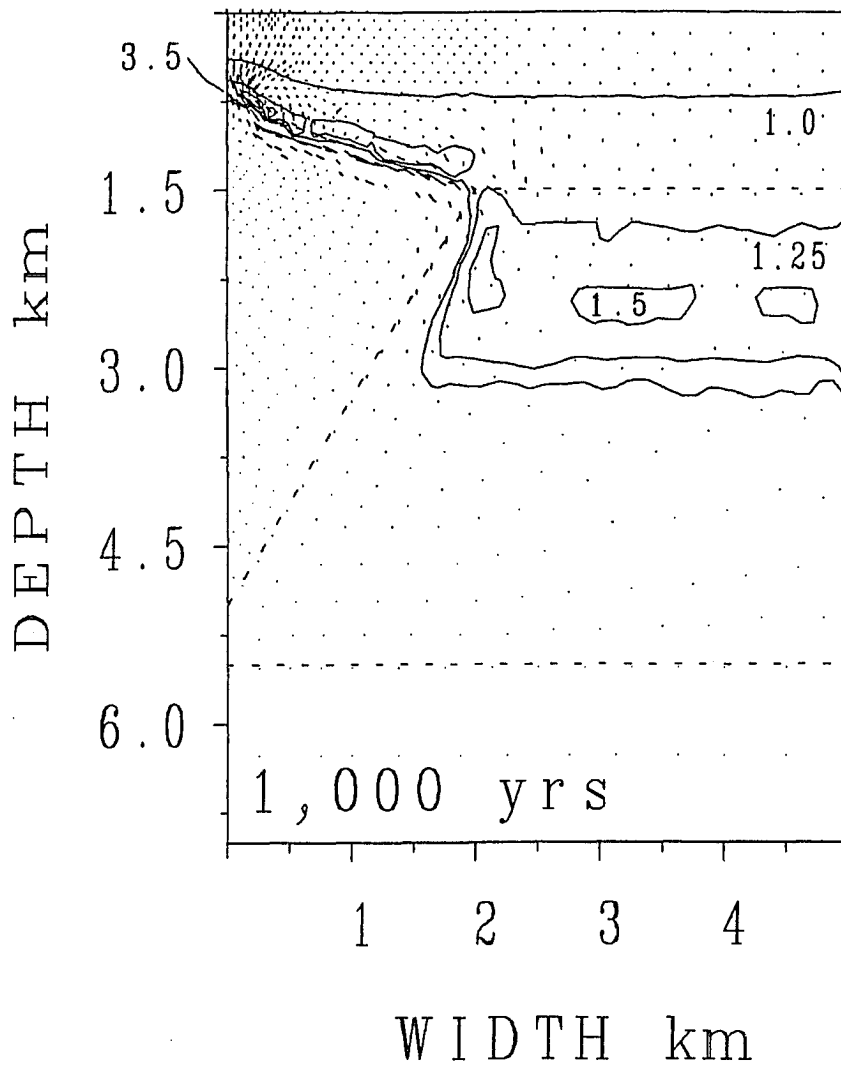


Figure 4: Narrow chamber : Fluid heat capacity and velocity at 1,000 yrs.

Contours indicate c_p values, velocity indicated by vectors in direction of fluid flow, length of vectors is proportional to the magnitude of v . Heat capacity reaches a sharp maximum at critical P-T conditions, and contours of c_p here outline the zone of near-critical conditions. Maximum fluid velocity at this time is 4.3×10^{-7} cm/sec.

impermeable. Localized high velocities immediately above the chamber result in rapid convective heat transport during this time, displacing isotherms upward, and compressing them toward the surface. The 100–200°C isotherms are visibly displaced at 10,000 years, and by 20,000 years they reach their closest approach to the surface. Distally, these same contours are displaced downward by the downflow portion of the circulation system.

By 20,000 years a sharp inflection in the geotherm develops at the location of the critical P–T conditions for H_2O (Fig.6), reflected by the roughness in the 400°C contour (Fig.5). The inflection forms at this location as a result of the tremendous increase in convective heat transport. This feature is a natural consequence of the properties of H_2O and the laws governing heat transport, and is formed by two segments of the geotherm that are controlled by low to moderate convection of heat, joined by a short segment where state conditions are near-critical and heat convection is extreme. This extreme is primarily the result of increased c_p of the fluid, figure (5) shows that fluid velocities are only moderately higher in this zone.

The zone of high velocities seen in fig.4 expands rapidly upward during this time (compare with fig.5), but remains very close to the ridge axis. The location of the zone is also indicated by the maximum contour of time-integrated mass flux at the ridge axis, and is always centered on the region of critical conditions ($\sim 350^\circ C$ at these pressures). Throughout this time period fluid upflow in the basalts is concentrated in a narrow zone within 1.5 km of the ridge axis by the influence of the critical P–T zone. A large circulation cell forms in the high-permeability basalts and dikes by 5,000 years, and gradually extends to greater depths as distal fluids begin to move toward the region of rapid upflow. The center of this cell remains just above the distal tip of the intrusion. Downflow rapidly

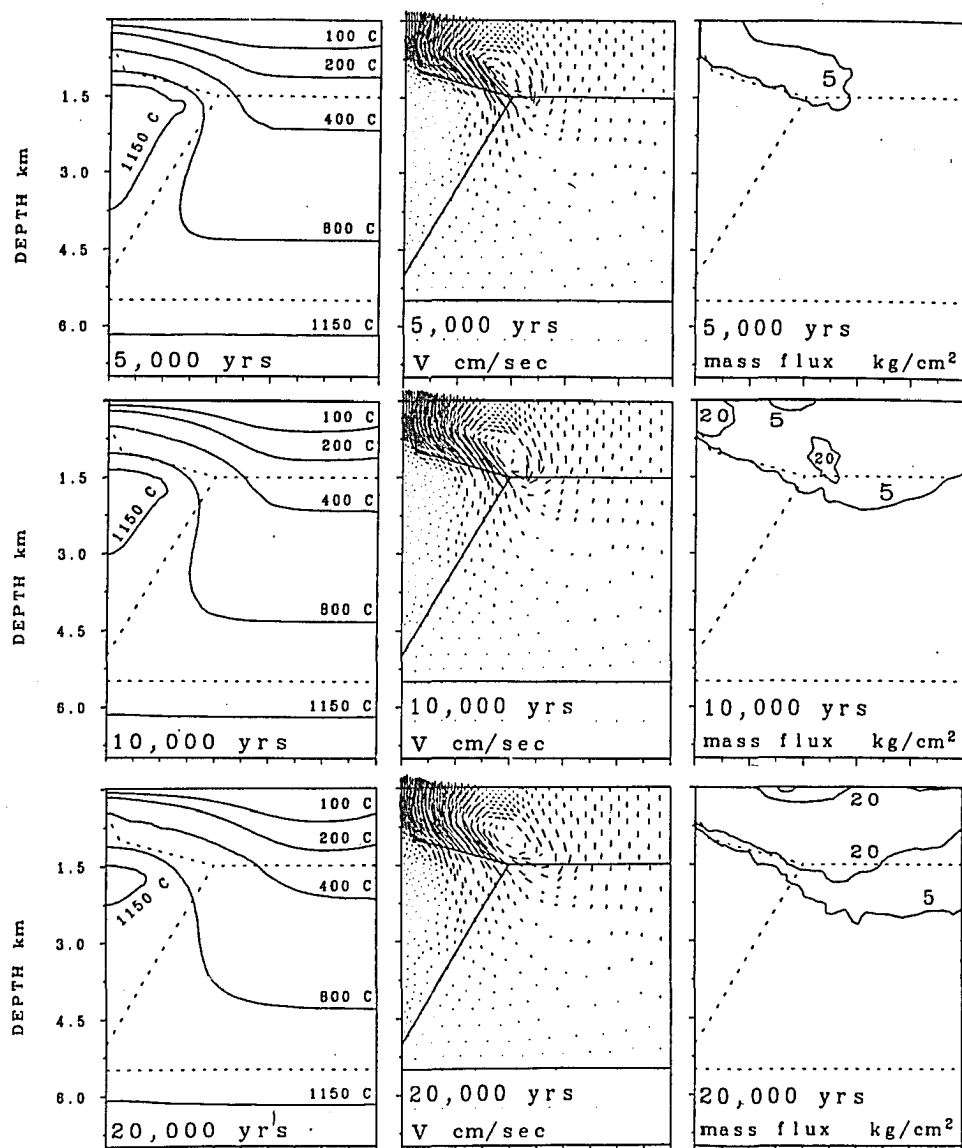


Figure 5: Narrow chamber: T contours, v vectors, and time-integrated mass flux contours for selected times.

The 1150°C contour represents the boundary of the magma. Length of velocity vectors is proportional to the magnitude of v .

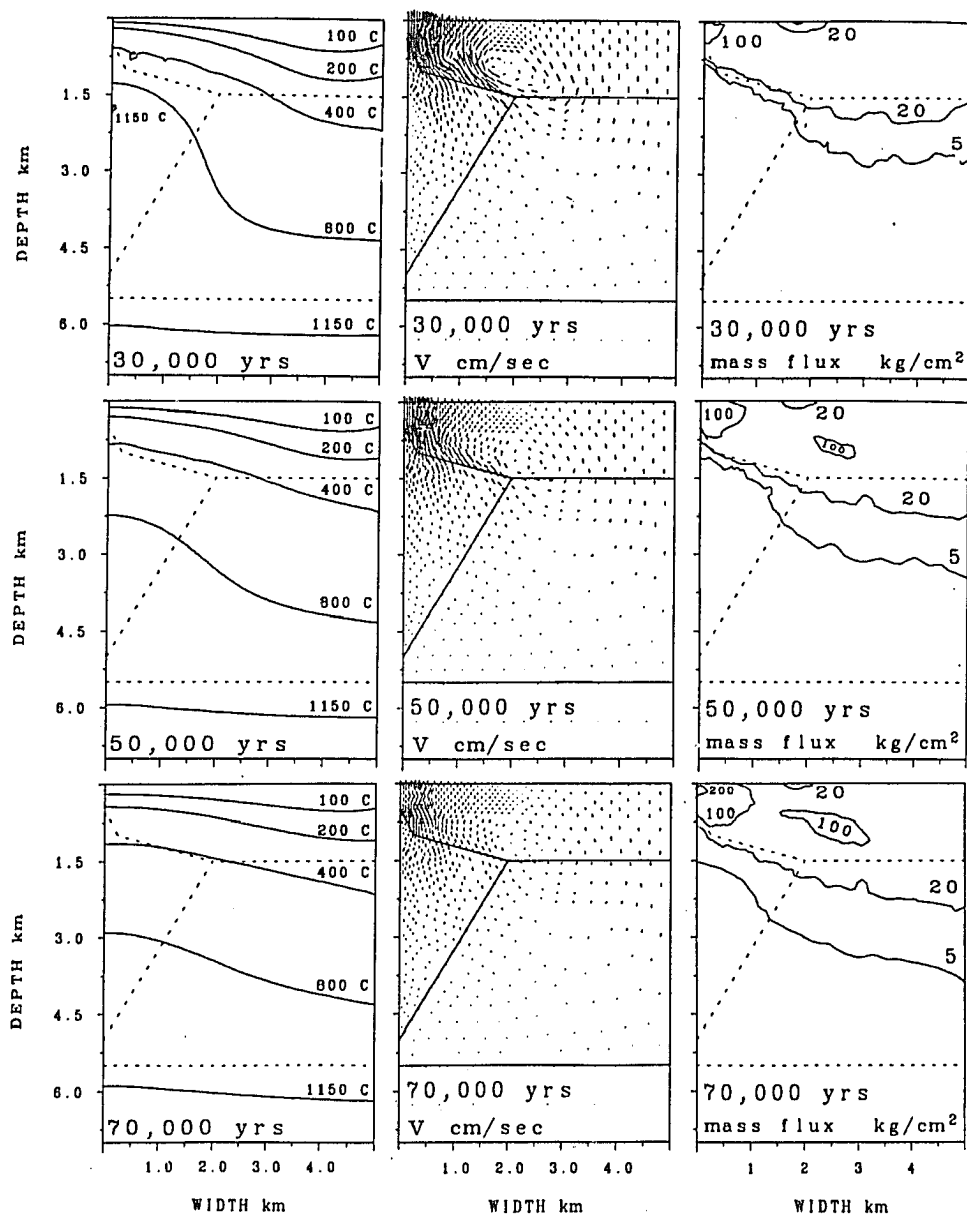


Figure 5: Continued.

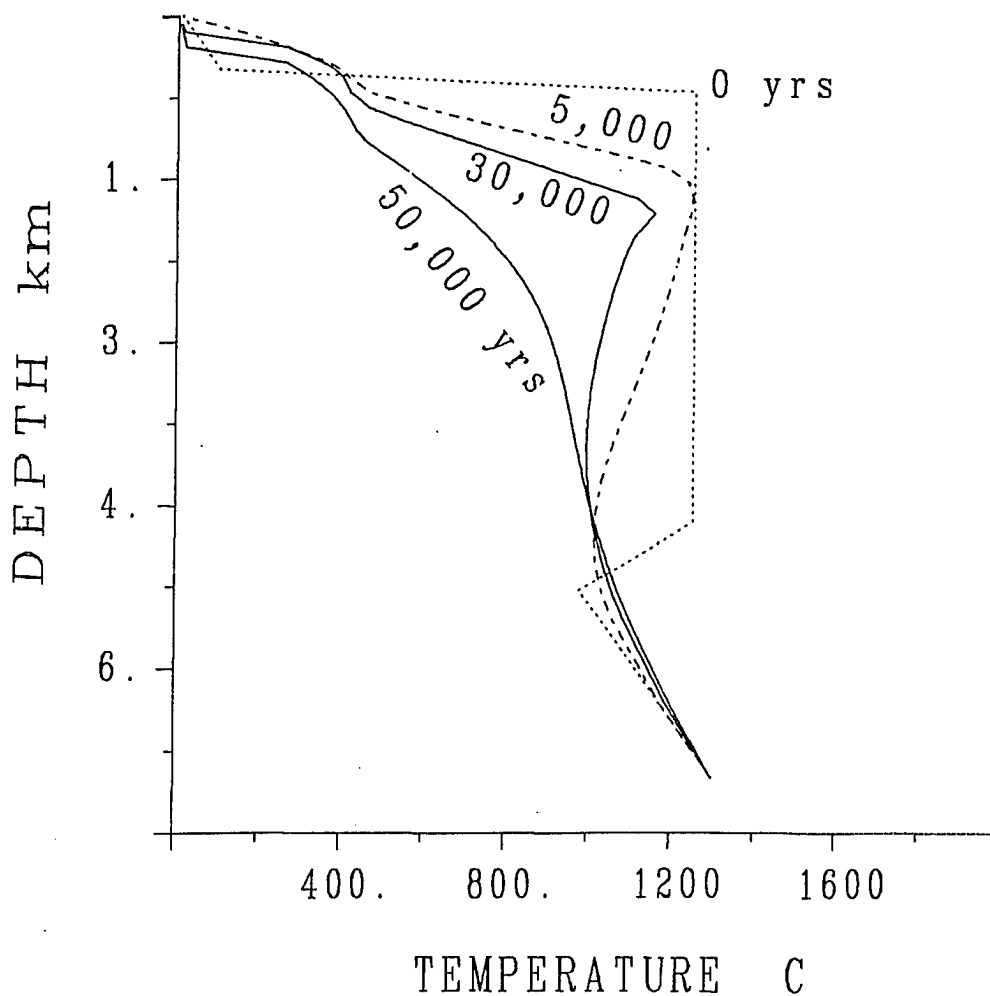


Figure 6: Narrow chamber : Temperature vs. depth at the ridge axis.

Note inflection in geotherm at 1/2 km depth, coinciding with the zone of critical P-T conditions and the top contact of the intrusion. Geotherms are skewed at ~ 1 km depth owing to concentration of crystallization heat at that depth.

increases in magnitude and extent during this period, and by 20,000 years the downward limb of the circulation pattern extends the full thickness of the crust. Time-integrated mass flux reaches high values in the upper parts of the gabbro by 20,000 years.

At 10,000 years mass flux at the surface reaches a maximum (Fig.3). Peak velocities at the surface at this time are about 4×10^{-7} cm/sec corresponding to a true velocity of about 1×10^{-3} cm/sec in flow channels. If the flow porosity over an area of 6×10^4 m² (i.e. a square 250 m on a side) were channeled into a single vent, fluid velocities would be equivalent to the maximum values reported for sea floor hot springs (2.4 m/sec, Converse, et al. 1984). This area is roughly consistent with the spacing of vent clusters in known vent fields, but suggests that groups of high velocity vents must be fed by vertically extensive zones of enhanced permeability.

30,000–50,000 yrs

Only a trace of magma remains by 30,000 years, and the intrusion is completely crystallized by 35,000 years. After 25,000 years, isotherms begin to move downward as convective heat transfer slowly declines throughout the system. The zone of hydrothermal outflow remains narrow at the surface, but with the retreat of the zone of critical conditions downward hot spring activity rapidly declines. After 30,000 years the entire intrusion becomes permeable, and fluid flow is chiefly vertical throughout the intrusion. Fluid flow in the gabbros continues at relatively high rates during this period, and time-integrated mass flux nears its final values by 50,000 years.

50,000–70,000 yrs

Isotherms continue to collapse downward during this time and the zone of

maximum velocities continues to retreat toward the intrusion. The concentration of upflow at the ridge axis produces a strong maximum in integrated mass flux there, while mass flux associated with downflow produces a secondary maximum at the distal tip of the intrusion. Relatively high values (5 kg/cm^2) of integrated mass flux extend to 4 km depth by 70,000 yrs. Although determining the extent and degree of alteration is not possible without a transport model, it is worth noting that similar values of fluid flux were sufficient to produce the observed alteration at the Skaergaard Intrusion (Norton and Taylor 1979). The temperature anomaly associated with the intrusion has cooled to one-third its original value by 70,000 yrs, and throughout the system convective heat transport has declined to low values (Fig.3).

Summary

1. The magma crystallizes completely in 30,000 yrs
2. Fluid upflow in the roof rocks and hot spring activity at the surface is restricted to a narrow 1 km wide zone immediately adjacent to the ridge axis for the lifetime of the system
3. Fluid flux at the surface increases rapidly with time, reaches a maximum at 15,000 years, after most of the magma has crystallized, then declines slowly
4. Mass flux integrated over the lifetime of the system is high through the full thickness of the crust, but is distributed non-uniformly in the roof rocks. The potential for significant rock alteration exists to depths of at least 4 km

5. The lifetime of the hydrothermal system (as defined by the time required to dissipate two-thirds of the initial thermal anomaly) is 70,000 yrs, more than twice that of the magma

CHAPTER 4

WIDE CHAMBER

The wide sill-like chambers proposed from ophiolite data imply much more broadly distributed thermal input into the ridge environment than in the narrow case, and therefore should develop a much more dispersed hydrothermal system. A cross-section presented by Pallister & Hopson (1981) is the basis for this model, slightly modified to include the same thickness of roof rocks as in the narrow case. The magma chamber extends 15 km away from the ridge axis, tapering from 4 km in height at the axis to a point at its distal end (Fig.7). Initial and boundary conditions (Fig.8) are identical to those for the narrow chamber. Heat sources were concentrated between 1.5 and 3.0 km depth for this model. The problem domain was divided into 430 elements using 909 nodes, 225 time steps were required to complete the solution.

P-T-v History

The history of hydrothermal circulation in this system can also be divided into three stages, although the history of convective heat and fluid flux at the surface is more complicated than in the narrow case (Fig.9). From 0-30,000 fluid flux increases rapidly in the basalts and at the surface, from 30,000-70,000 it reaches its peak and remains relatively high, and from 70,000-170,000 fluid flux decreases slowly, reaching very low values by 170,000 years.

Narrow cross-section

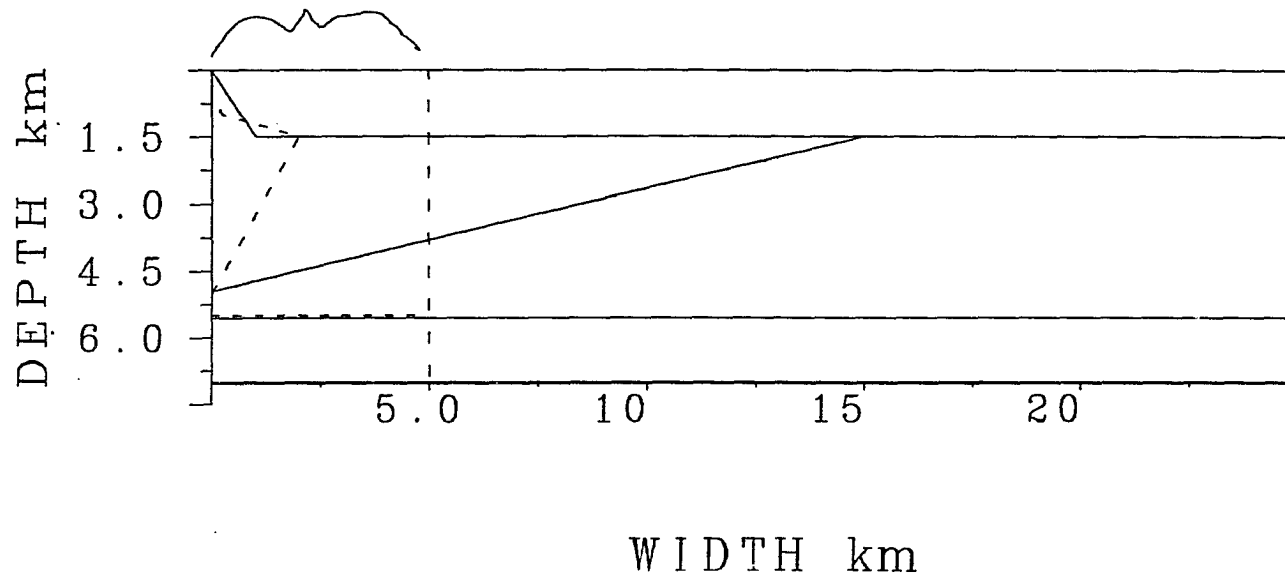


Figure 7: Comparison of initial geometries, wide and narrow chambers.
Dashed lines show outline of narrow chamber cross-section.

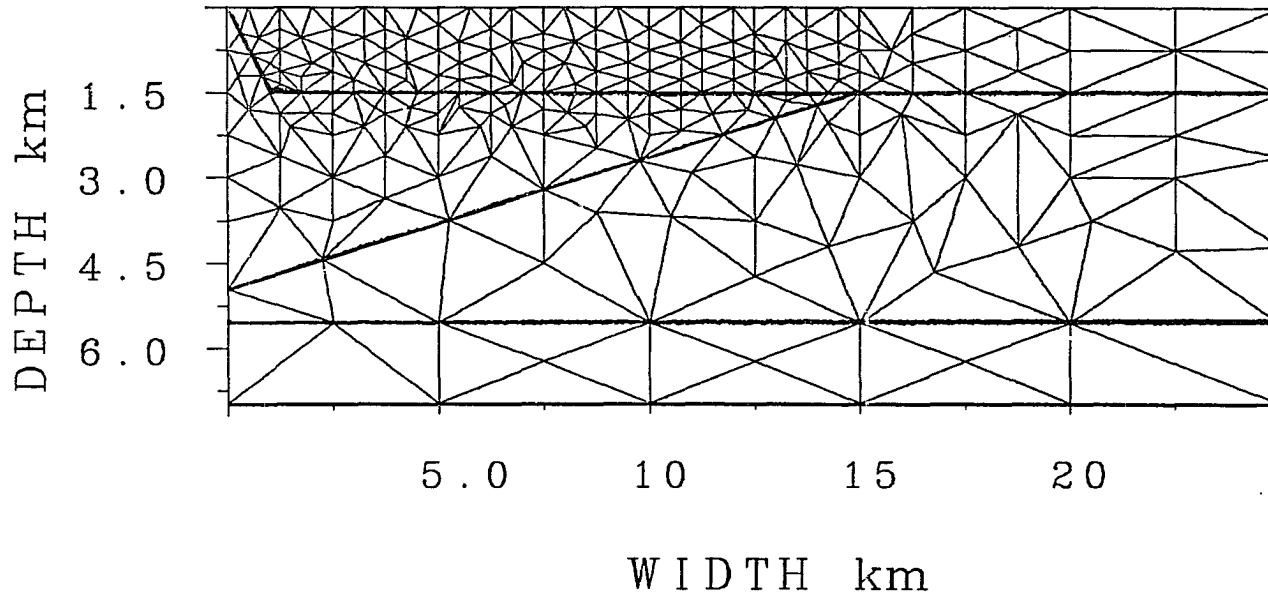


Figure 8: Wide chamber : Element grid.

Boundary and initial conditions are identical to those in the narrow model.

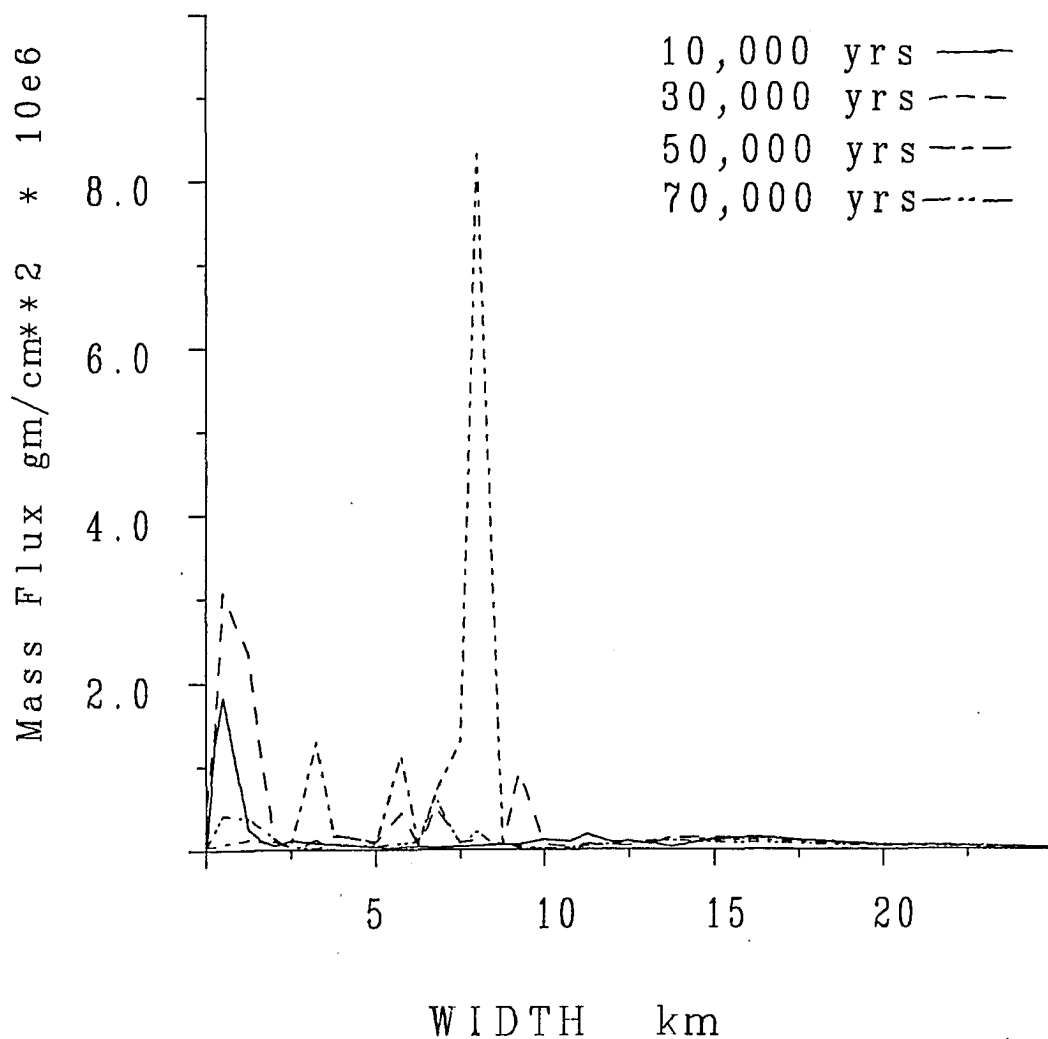


Figure 9: Wide chamber : mass flux at the ocean floor for selected times.

Instantaneous mass flux ($\rho \cdot |v|$) at 10,000, 30,000, 50,000 and 70,000 years. Note that the flux is periodic in space but irregular in time, and that peak fluxes are found well off axis.

0-30,000 yrs

A broad zone of high fluid velocities forms by 10,000 years, located immediately above the magma chamber where P-T conditions are near-critical (Fig.10). Several small convection cells associated with this critical zone form in the permeable layer above the magma chamber, with a small but vigorous cell appearing at the ridge axis (Fig.11). This circulation cell develops just above a set of intrusive 'dikes' (the small triangular extension of the magma chamber at the ridge axis), and disappears after the dikes have cooled (by 30,000 years).

Rapid solidification of the magma takes place at the distal tip of the intrusion in response to high conductive heat transport where surface area is large. About one-fifth of the intrusion is solid by 10,000 years, and two-fifths by 30,000 years. During this period most of the intrusion remains impermeable, and only at the distal tip can fluids move upward from the gabbros into the basalts. As a result, the equivalent of the large circulation cell found near the ridge axis in the narrow case forms far from the axis at the distal tip of the wide chamber. Nearer the ridge axis only small cells form, isolated from the gabbros by the impermeable magma. Just above the magma chamber strong fluid influx into the broad critical zone, combined with the presence of the impermeable magma, channels flow into a narrow band of chiefly horizontal flow at the base of the basalts. This band extends above the full length of the magma chamber at 10,000 years, but begins to break down by 30,000 as the region of critical conditions expands, and fluids at the base of the basalt more buoyant and travel upward instead.

The scale of this model makes it more difficult to resolve the effects of convection in the isotherms. Small displacements in the 200-400°C contours at

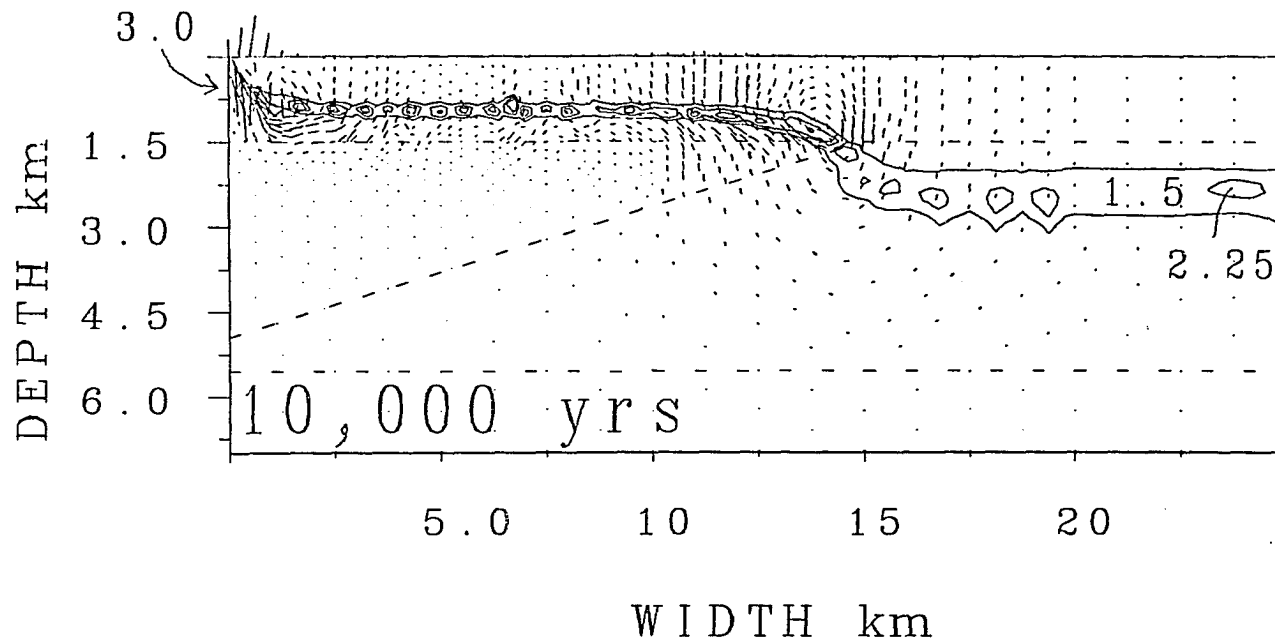


Figure 10: Wide chamber : Fluid heat capacity contours and v at 10,000 yrs.

Fluid c_p contours indicate the zone of near-critical P-T conditions. Length of velocity vectors is proportional to the magnitude of v . Maximum velocity at this time is 2.2×10^{-7} cm/sec.

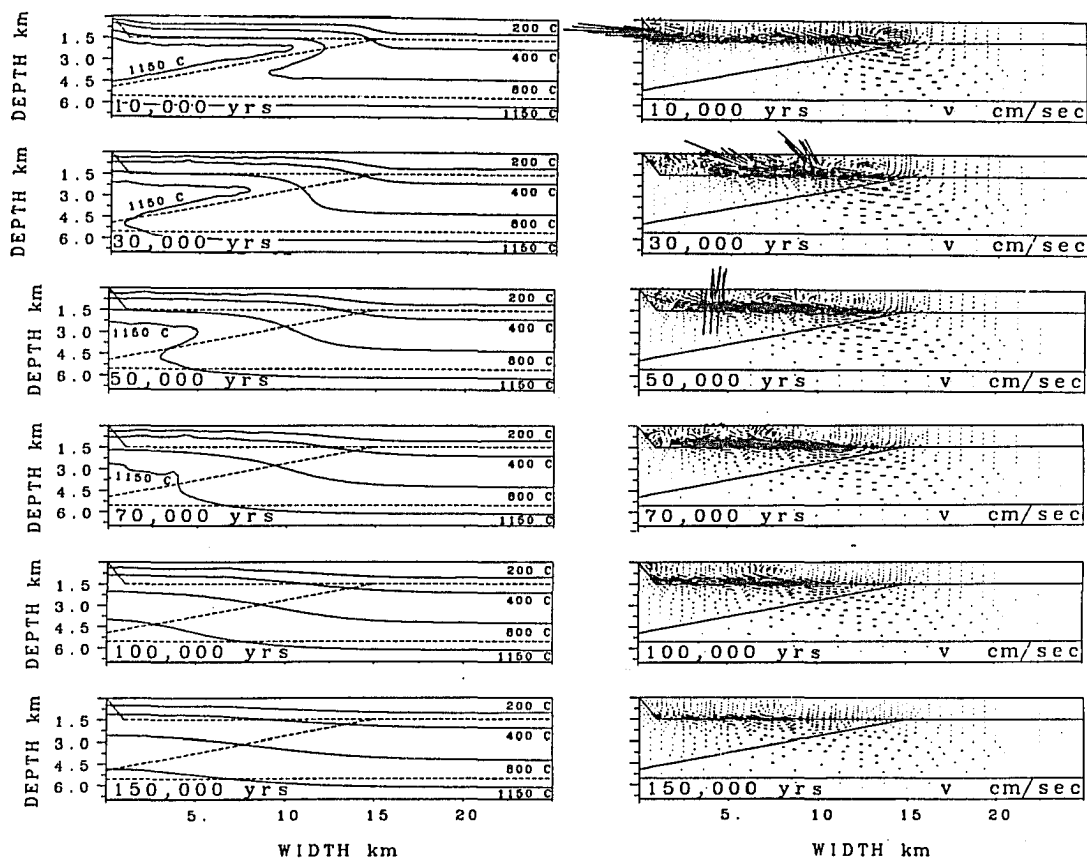


Figure 11: Wide chamber: T contours, v vectors, time-integrated mass flux and streamfunction contours at selected times.

The 1150°C contour represents the boundary of the magma. Length of velocity vectors is proportional to the magnitude of v . Streamfunction is a function of ∇v , and its contours are tangent to fluid flow vectors (i.e. contours are streamlines) while their spacing is inversely proportional to fluid velocity.

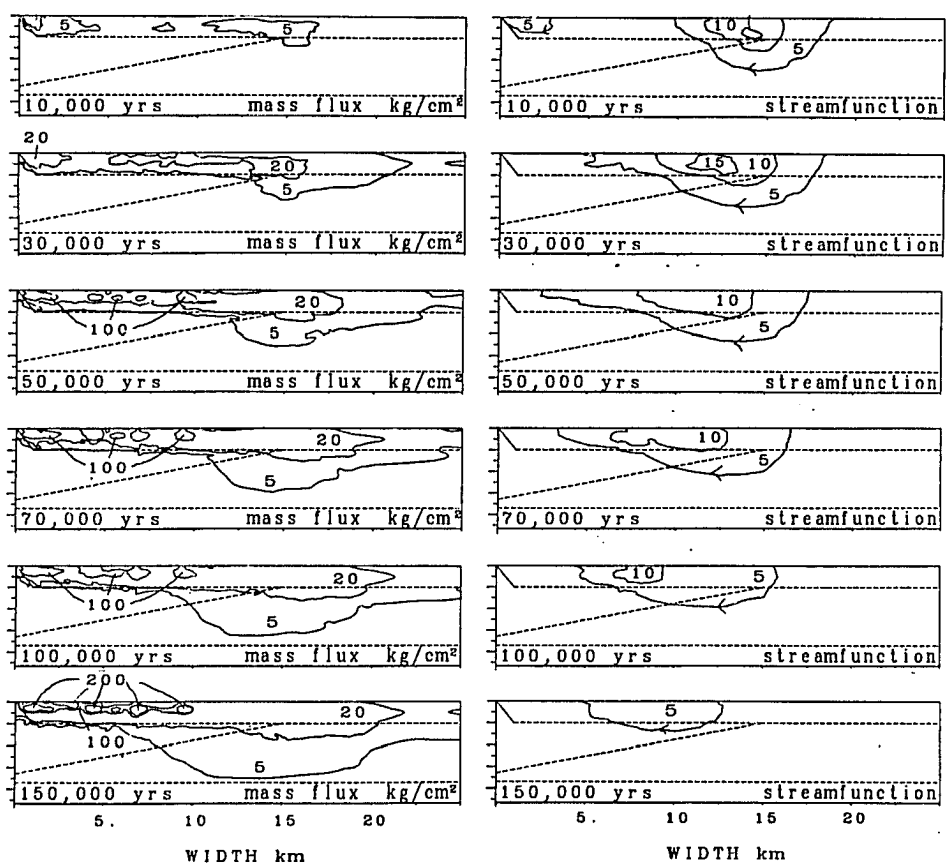


Figure 11: Continued.

30,000 years are the product of the small circulation cells in the basalts. Distal to the tip of the magma chamber, the 200°C contour is depressed slightly by 30,000 years. Because of the transient nature of the small circulation cells in the basalts, no sharp jump in the geotherm develops above the intrusion, in contrast to the narrow case. The flat contours of integrated mass flux reflect the rapid onset of circulation throughout much of the basalts, but because it depends on fluid density as well as velocity, mass flux is actually highest just above the zone of maximum velocities. By 30,000 integrated mass flux has reached quite high values in parts of the basalts, and moderate values in the upper gabbros at the tip of the intrusion.

30,000-70,000 yrs

During this period, the liquid portion of the intrusion continues to retreat rapidly away from the distal tip of the chamber, obtaining a shape similar to that of the narrow chamber by 50,000 years. At 50,000 years about one-fifth of the intrusion remains liquid, by 70,000 years only 10% remains. With the retreat of the solidus isotherm, more of the distal portion of the intrusion becomes permeable, and the large circulation cell at the intrusion tip begins to involve rocks closer to the ridge axis. By 70,000 years the distal 10 km of the intrusion have become permeable and are affected by fluid flow.

The effects of convection on the temperature contours remains visible, with small upward and downward displacements appearing at 50,000 and 70,000 years. Distal depression of the 200°C contour is faintly visible at 70,000 years. During this time period critical conditions make their closest approach to the surface, appearing within 500 m of the surface at 50,000 years. This is also the time of maximum surface fluid flux (Fig.9).

Velocities in the portion of the large circulation cell affecting the gabbros increase during this period. As the large cell increases in size, its center moves toward the axis as well, in response to the retreat of the impermeable portions of the intrusion. The magnitude of horizontal flow at the base of the basalts begins to decrease and the band moves toward the axis as the permeability barrier formed by the magma shrinks toward the ridge axis. Integrated mass flux contours have reached near-final values in the basalts by 70,000 years, and extend deep into the distal gabbros by this time as well.

70,000–170,000 years

The magma has completely solidified by 120,000 years. Near-solidus temperatures in the lower crust stabilize the final melt fraction in this area. Given the high background geothermal gradient this distribution of final melt was unavoidable without extreme concentration of heat sources at the top of the intrusion. Soon after 70,000 years the entire upper portion of the intrusion is permeable, and fluids in the intrusion begin to flow laterally and upward toward the basalts. After 70,000 the isotherms begin to retreat slowly downward as the magnitude of convection declines. Some displacements are present in the 200°C contour at 100,000 years, the last local effects of convection visible in this model.

The zone of horizontal flow at the base of the basalts reaches the ridge axis at 100,000 years, and surface flux at the axis increases for a short time as a result. Before this time, surface mass flux at the ridge axis is inhibited by the low permeability of the intrusion. The large circulation cell affects the entire intrusion and most of the underlying gabbros by 100,000 years. High integrated mass flux values are found in the gabbros below the intrusion tip, and moderate values are present in the upper mantle rocks as well. Final integrated mass flux values are

sufficient to produce significant rock alteration throughout the crust and upper portion of the mantle as well. By 170,000 years, the average temperature of the intrusion has cooled to one-third its initial value, and the system returns to a conduction-dominated state.

Summary

1. The magma crystallizes completely in 100,000 years
2. Several small but vigorous convection cells form in the basalts above the intrusion. Maximum integrated mass fluxes associated with these cells are distributed irregularly in the basalts
3. A large convection cell forms at the distal tip of the intrusion, and gradually moves inward and engulfing the small cells in the basalts as the intrusion becomes permeable
4. Surface fluid flux occurs over a broad zone extending 10 km from the ridge axis and is high from 50,000 to 100,000 years
5. Surface fluid flux reaches a maximum at 50,000 years 10 km away from the ridge axis, but peaks at 100,000 years for vents at the axis
6. High values of integrated mass flux are found in the gabbros below the tip of the intrusion, and moderate values extend below the gabbros into the mantle rocks, with potential for significant rock alteration throughout the thickness of the crust and uppermost mantle
7. The system cools to $1/3$ the original thermal anomaly by 170,000 years

CHAPTER 5

DISCUSSION

The models presented above demonstrate that profoundly different hydrothermal systems will develop around the two extremes of proposed magma chamber geometry. By itself this is not a novel conclusion, given a larger more broadly distributed magma chamber, a broader and more vigorous hydrothermal system forms; however, an important underlying principle emerges from comparison of the two models. The development of a zone of critical conditions is the basic driving mechanism in mid-ocean ridge hydrothermal systems, and the form of this zone controls the pattern and evolution of hydrothermal circulation. The different chambers produced different patterns of critical T-P conditions, and that led to profoundly different hydrothermal systems. Given an understanding of this driving mechanism, the style of hydrothermal circulation around any proposed magma chamber can be predicted. In addition, the influence of factors such as multiple intrusions and sea-floor spreading can be evaluated by considering their interaction with the zone of critical conditions.

Two other general features of mid-ocean ridge hydrothermal systems are clear in the above models. The first is that there is a significant delay between the intrusion of magmas and the peak of hydrothermal activity at the surface. This delay is directly proportional to the thickness and permeability of the roof rocks, and is a consequence of the time required for fluids to travel from the top of the chamber to the surface. A second important feature is that hydrothermal activity

at and below the surface persists for nearly twice the lifetime of the magma. Both these features serve to weaken the correlation between surface hot-spring activity and active magma chambers, indicating that vigorous hot-springs are not necessarily indicators of liquid magma in the sub-surface.

Both models yielded values of time-integrated mass flux of at least 5 kg/cm² through most of the gabbros, and up to 2 kg/cm² in the upper mantle rocks for the wide chamber. The wide chamber produces more fluid flow in the deep rocks because of its larger upflow zone, larger net hydrothermal outflow, and consequently greater demand for resupply from the deep crustal rocks. Since these magnitudes of integrated flux are similar to those modeled by Norton & Taylor (1979) for the Skaergaard Intrusion, it appears that chemical and isotopic alteration of the entire thickness of oceanic crust is achieved at the ridge (as proposed by Gregory & Taylor, 1981).

Spreading and Multiple Intrusions

Several potentially serious simplifications are made in the above models, perhaps the most important was the omission of the effects of sea-floor spreading and multiple intrusions. Fortunately, lateral transport of heat and material owing to sea-floor spreading, as well as multiple injections of magma at the ridge axis would have only minor effect on the results, serving primarily to reinforce the patterns of hydrothermal activity observed in the simplified models. The principal effect of spreading on the wide chamber would be to carry the zone of critical conditions and impermeable parts of the intrusion farther away from the ridge axis, further broadening the zone of fluid upflow. In the case of the narrow chamber the conditions that focus upflow near the ridge axis would be extended away from

the axis, but only by a short distance since little horizontal movement can take place in the brief lifetime of the narrow hydrothermal system.

An added effect of sea-floor spreading would be to reduce horizontal fluid velocities (which are chiefly ridgeward in the models) by the speed of the spreading plate. In the gabbroic rocks, fluid velocities are of the same order of magnitude as typical plate velocities, and therefore relative to a fixed frame of reference horizontal fluid velocities could be near zero in the lower crust. This would emphasize the primarily vertical flow seen in the narrow model, and reduce the degree of horizontal transport in the wide model.

The principal effect of multiple intrusive events on the model results would be to raise the background geothermal gradient present at the beginning of each intrusive cycle. This alone would have little influence on the patterns of hydrothermal activity, but the reinforcement of the impermeable zone created by the magma would deflect deep fluid flow away from the ridge axis. For the narrow chamber, this deflection would be too small to affect the distribution of surface fluid flux, but for the wide chamber the maximum surface fluid flux would be displaced farther from the ridge axis.

Fracture Zones

Another serious assumption is that permeability is uniform and homogeneous in each rock unit. The influence of such zones depends chiefly on how they interact with the zone of critical conditions. Fractures reaching the surface would strongly control the location of hot springs (see Fehn & Cathles, 1979; Little, 1987) but their influence on sub-surface flow depends largely on whether they intersect the zone of critical conditions. If fractures extend from the surface into or beyond

the zone of critical conditions they will form the major pathways of fluid flow (both upward and down) and may have a major effect on the entire flow field. If on the other hand fractures do not reach the zone of critical conditions, they will influence only the local flow field, and not the general circulation pattern. This is because they would have little effect on the distribution of critical conditions, or on the movement of fluid into and out of the critical zone.

CHAPTER 6

CONCLUSIONS

The models in this study establish a first-order relation between magma chamber geometry and the patterns of hydrothermal activity at mid-ocean ridges. Two extremes of chamber geometry have been proposed in the literature, based on separate lines of evidence. Petrologic evidence seems to demand a wide chamber, and if such chambers are present at the ridge axis significant levels of off-axis hydrothermal activity will take place, including hot springs and alteration of crustal rocks. If the distal parts of these chambers have an appreciable thickness (≥ 1 km), off-axis hot springs will be longer lived and vent much greater quantities of fluid than their on-axis counterparts. Seismic data at the ridge axis may not rule out wide chambers, since the distal portions of such chambers will cool rapidly, resulting in a narrow-like chamber for the latter two-thirds of the lifetime of a wide chamber.

In contrast, if the petrologic evidence can somehow be dismissed, then the seismic data could be accepted at face value as limiting possible chambers to less than 2 km width. Hydrothermal activity related to such chambers will be tightly focused along the ridge axis, consistent with current data indicating detectable surface hydrothermal activity is restricted to a narrow zone at the axis.

True ridge chambers may be some hybrid or intermediate between the extremes modeled above. In general, any chamber or series of chambers that produce a zone of critical conditions sloping upward toward the ridge axis will

produce a focused zone of upflow and hot spring activity. Chambers that produce a wide flat critical zone will produce wide regions of upflow and hot spring activity. Strong hydrothermal circulation in the gabbros will be found outside the distal end of all but the narrowest chambers.

The relation between chamber geometry and pattern of hydrothermal activity is almost entirely a function of the distribution of critical T-P conditions. This concept can be applied without further resort to numerical modeling to predict the general nature of sub-surface hydrothermal activity for any given form or combination of magma chambers at the mid-ocean ridge. Given the current state of knowledge about ridge geology, and particularly about magmatism and rock permeability, only this kind of general result can be obtained from numerical modeling. Hopefully as more detailed information becomes available, more accurate simulations of the ridge environment will be possible.

APPENDIX A

GLOSSARY OF SYMBOLS

<u>English Symbols</u>	<u>Meaning</u>	Units	
		<u>CGS</u>	<u>SI</u>
c_p	isobaric heat capacity	cal/gr°C	J/gr°C
g	gravitational constant	cm/sec ²	m/sec ²
\mathbf{g}	gravitational force vector	cm/sec ²	m/sec ²
k	rock permeability	cm ²	m ²
P	total pressure	barye	pascal
Q_{zi}	latent heat of crystallization	cal/cm ³ °C	J/m ³ °C
T	temperature	°C	°C
T_f	fluid temperature	°C	°C
T_s	rock temperature	°C	°C
\mathbf{v}	Darcy velocity vector	cm/sec	m/sec
v_i	velocity component in the i th direction	cm/sec	m/sec
x_i	coordinate in the i th direction	cm	m
z	vertical coordinate (positive upward)	cm	m

<u>Other Symbols</u>	<u>Meaning</u>	<u>Units</u>	
		<u>CGS</u>	<u>SI</u>
Δt	time step	sec	sec
Δx_i	space step in i th direction	cm	m
κ	thermal diffusivity	cm ² /sec	m ² /sec
μ	dynamic viscosity	gm/cm sec	kg/m sec
ϕ	porosity		
ρ	rock density	gm /cm ³	kg / m ³
ρ_f	fluid density	gm /cm ³	kg / m ³

REFERENCES

- Anderson, R.N., M.D.Zoback, S.H.Hickman and R.L.Newmark, 1985. Permeability versus depth in the upper oceanic crust : In-situ measurements in DSDP hole 504B, Eastern Equatorial Pacific. *J. Geophys. Res.*, 90:3659-3669
- Becker, K., M.G. Langseth, R.N. Anderson and M.A. Hobart, 1985. Deep crustal geothermal measurements, hole 504B, Deep Sea Drilling Project legs 69, 70, 83 and 92. Initial Rep. Deep Sea Drill. Proj., 83:405-418
- Bowers, T.S. and H.P. Taylor, 1985. An integrated chemical and isotopic model of the origin of mid-ocean ridge hot springs systems. *J. Geophys. Res.*, 90:12583-12606
- Bryan, W.B. and J.G.Moore, 1977. Compositional variations of young basalts in the Mid-Atlantic Ridge rift valley near lat 36°40' N. *Geol. Soc. Amer. Bull.*, 88:556-570
- Cathles, L.M., 1983. An analysis of the hydrothermal system responsible for massive sulfide deposition in the Hokuroku Basin of Japan. In: *The Kuroko and Related Volcanogenic Massive Sulfide Deposits*, *Econ. Geol. Mono.*, 5:439-450
- Converse, D.R., H.D. Holland and J.M. Edmond, 1984. Flow rates in the axial hot springs of the East Pacific Rise (21° N): Implications for the heat budget and the formation of massive sulfide deposits. *Earth Planet. Sci. Lett.*, 69:159-175

- Corliss, J.B., J. Dymond, I. Gordon, J.M. Edmond, R.P. von Herzen, R.D. Ballard, K. Green, D. Williams, A. Bainbridge, K. Crane and T. van Andel, 1979. Submarine thermal springs on the Galapagos Rift. *Science*, 207:1421-1433
- Detrick, R., P. Buhl, J. Mutter, J. Orcutt, T. Brocker, J. Madsen, 1986. Multi-channel seismic imaging of the axial magma chamber along the East Pacific Rise between 9°N and 13°N [Abstr]. *EOS*, 67:360
- Fehn, U. and L.M. Cathles, 1979. Hydrothermal convection at slow-spreading mid-ocean ridges. *Tectonophysics*, 55:239-260
- Francheteau, J. and R.D. Ballard, 1983. The East Pacific Rise near 21°N, 13°N, and 20°S : Inferences for along-strike variability of axial processes of the mid-ocean ridge. *Earth and Plan. Sci.*, 64:93-116.
- Gartling, D.K., 1982. Finite element analysis of thermal convection in deep ocean sediments. *Adv. Water Resour.*, 5(3):136-141
- Gartling, D.K. and C.E. Hickox, 1983. MARIAH-A finite element computer program for incompressible porous flow problems : User's manual. Sandia National Labs Rept., 79-1623:
- Gregory, R.T. and H.P. Taylor, 1981. An oxygen isotope profile in a section of Cretaceous oceanic crust, Semail Ophiolite, Oman : Evidence for δO^{18} buffering of the oceans by deep (> 5 km) seawater-hydrothermal circulation at mid-ocean ridges. *J. Geophys. Res.*, 86:2737-2755
- Gregory, R.T., 1984. Melt percolation beneath a spreading ridge : evidence from the Semail peridotite, Oman. *Ophiolites and Oceanic Lithosphere*, pp. 55-62

- Harr, L., J.C. Gallagher, and G.S. Kell, 1984. NBS/NRC Steam Tables. Washington, D.C., Hemisphere Pub., 320 pp.
- Huyakorn, P.S. and G.F. Pinder, 1983. Computational methods in subsurface flow. J. Wiley and Sons, New York, 473 pp.
- Knapp, R.B. and D. Norton, 1981. Preliminary numerical analysis of processes related to magma crystallization and stress evolution in cooling pluton environments. *Am. J. Sci.*, 281:35-68
- Langmuir, C.H., J.F. Bender, and R. Batiza, 1986. Petrological and tectonic segmentation of the East Pacific Rise 5°30' – 14°30'N. *Nature*, 322:422-429
- Lapidus, L. and G.F. Pinder, 1982. Numerical solution of partial differential equations in science and engineering. John Wiley and Sons, New York, 677 pp.
- Levelt Sengers, J.M.H., B. Kamgar-Parsi, F.W. Balfour, and J.V. Sengers, 1983. Thermodynamic properties of steam in the critical region. *J. Phys. Chem. Ref. Data*, 12(1):1-28
- Lewis, B.T.R., 1983. The process of formation of ocean crust. *Science*, 220:151-157
- Lister, C.R.B., 1972. On the thermal balance of a mid-ocean ridge. *Geophys. J. Roy. Astron. Soc.*, 26:515-535
- MacDonald, K.C., 1982. Mid-ocean ridges : Fine scale tectonic, volcanic and hydrothermal processes within the plate boundary zone. *Ann. Rev. Earth Plan. Sci.*, 10:155-190

- MacDonald, K.C., 1986. The crest of the Mid-Atlantic ridge: Models for crustal generation processes and tectonics. In: *The Geology of North America : The Western North-Atlantic Region*, M:51-68
- MacDonald, K.C., K.Becker, F.N.Speiss and R.D.Ballard, 1980. Hydrothermal heat flux of the 'black smoker' vents on the East Pacific Rise. *Earth Plan. Sci. Lett.*, 48:1-7
- MacDonald, K.C., J.C. Sempere, and P.J. Fox, 1984. East Pacific Rise from Sequiros to Orozco fracture zones: Along-strike continuity of axial neovolcanic zone and structure and evolution of overlapping spreading centers. *J. Geophys. Res.*, 89:6049-6069
- McClain, J.S., J.A.Orcutt, and M.Burnett, 1985. The East Pacific Rise in cross-section : A seismic model. *J. Geophys. Res.*, 90:8627-8640
- Morton, J.L. and N.H.Sleep, 1985. A mid-ocean ridge thermal model : constraints on the volume of axial hydrothermal heat flux. *J. Geophys. Res.*, 90:11345-11353.
- Norton, D.L., 1984. Theory of hydrothermal systems. *Ann. Rev. Earth Planet. Sci.*, 12:155-177
- Norton, D.L., 1987. The mathematical theory of magma- hydrothermal systems. Unpubl. manuscript, 130p.
- Norton, D. and J.Knight, 1977. Transport phenomena in hydrothermal systems : cooling plutons. *Am. J. Sci.*, 277:937-981
- Norton, D. and H.P.Taylor, 1979. Quantitative Simulation of the hydrothermal systems of crystallizing magmas on the basis of transport theory and

- oxygen isotope data : An analysis of the Skaergaard Intrusion. *J. Petrol.*, 20:421-486
- Pallister, J.S. and C.A.Hopson, 1981. Samail ophiolite plutonic suite : Field relations, phase variation, cryptic variation and layering, and a model of a spreading ridge magma chamber. *J. Geophys. Res.*, 86:2593-2644
- Ribando, R.J., K.E.Torrance and D.L.Turcotte, 1976. Numerical models for hydrothermal circulation in the oceanic crust. *J. Geophys. Res.*, 81:3007-3012
- Roache, P.J., 1972. *Computational Fluid Dynamics*. Hermosa Publishers, Albuquerque, N.M, 446 pp.
- Rona, P.A., G. Klinkhammer, T.A. Nelson, J.H. Trefry and H. Elderfield, 1986. Black smokers, massive sulfides, and vent biota at the mid-Atlantic Ridge. *Nature*, 321:33-37.
- Rona, P., G.Thompson, M.J.Mottl, J.A.Karson, W.J.Jenkins, D.Graham, M.Malette, K.VonDamm and J.M.Edmond, 1984. Hydrothermal activity at the Trans-Atlantic geotraverse hydrothermal field, Mid-Atlantic Ridge crest at 26°N. *J. Geophys. Res.*, 89:11365-11377
- Shirey, S.B., J.F.Bender and C.H.Langmuir, 1987. Three-component isotopic heterogeneity near the Oceanographer transform, mid- Atlantic Ridge. *Nature*, 325:217-223
- Spooner, E.T.C., R.D.Beckinsale, P.C.England, and A.Senior, 1977. Hydration, O^{18} enrichment and oxidation during ocean floor hydrothermal metamorphism of ophiolitic metabasic rocks from E.Liguria, Italy. *Geochim. Cosmo. Acta*, 41:857-871

- Sleep, N.H., 1983. Hydrothermal convection at ridge axes. NATO Conference Series IV: Marine Sciences, 12:71-82
- Sleep, N.H. and B.R. Rosendahl, 1979. Topography and tectonics of mid-ocean ridge axes. J. Geophys. Res., 84:6831-6839
- Thompson, G., 1983. Basalt-seawater interaction. In: Hydrothermal Processes at Seafloor Spreading Centers [Rona, P.A., K. Bostrom, L. Laubier and K.L. Smith Jr., eds], NATO Conf. Series IV: Marine Sciences, 12:225-278
- Usselman, T.M. and D.S. Hodge, 1978. Thermal control of low- pressure fractionation processes. J. Volcanol. and Geother. Res., 4:265-281.
- Williams, C.F., T.N. Narasimhan, R.N. Anderson, M.D. Zoback and K. Becker, 1986. Convection in the oceanic crust: Simulation of observations from Deep Sea Drilling Project hole 504B, Costa Rica Rift. J. Geophys. Res., 91:4877-4889
- Williams, D.L., R.P. von Herzen, J.G. Sclater and R.N. Anderson, 1974. The Galapagos spreading center : Lithospheric cooling and hydrothermal circulation. Geophys. J. Roy. Astron. Soc., 38:587-608
- Wolery, T.J. and N.H.Sleep, 1976. Hydrothermal circulation and geochemical flux at mid-ocean ridges. J. Geol., 84:249-257